Accurate measurement of microscopic forces and torques using optical tweezers

Authors:
Melanie McLaren[1]
Elias Sidderas-Haddad[2]
Andrew Forbes[1,3]

Affiliations:
[1]National Laser Centre, CSIR, Pretoria, South Africa

[2]School of Physics, University of the Witwatersrand, Johannesburg, South Africa

[3]School of Physics, University of KwaZulu-Natal, Durban, South Africa

Correspondence to:
Andrew Forbes

Email:
aforbes1@csir.co.za

Postal address:
PO Box 395, Pretoria 0001, South Africa

Dates:
Received: 06 May 2009
Accepted: 12 May 2011
Published: 19 Sept. 2011

How to cite this article:
McLaren M, Sidderas-Haddad E, Forbes A. Accurate measurement of microscopic forces and torques using optical tweezers. S Afr J Sci. 2011;107(9/10), Art. #579, 8 pages. doi: 10.4102/sajs.v107i9/10.579

It is now well known that matter may be trapped by optical fields with high intensity gradients. Once trapped, it is then possible to manipulate microscopic particles using such optical fields, in so-called optical tweezers. Such optical trapping and tweezing systems have found widespread application across diverse fields in science, from applied biology to fundamental physics. In this article we outline the design and construction of an optical trapping and tweezing system, and show how the resulting interaction of the laser light with microscopic particles may be understood in terms of the transfer of linear and angular momentum of light. We demonstrate experimentally the use of our optical tweezing configuration for the measurement of microscopic forces and torques. In particular, we make use of digital holography to create so-called vortex laser beams, capable of transferring orbital angular momentum to particles. The use of such novel laser beams in an optical trapping and tweezing set-up allows for the control of biological species at the single-cell level.

Introduction

Microscopic forces are generally difficult to quantify as their effects are not experienced at the macro level. This difficulty places great limitations on fields such as cell biology and microfluidics, where much research is performed on the microscopic scale. Optical tweezing is an accurate and non-invasive method of measuring not only microscopic forces but also the torques experienced by microparticles, providing numerous applications within fields such as biology,[1,2,3,4] microfluidics[5,6] and aerosol dynamics.[7]

Ashkin and co-workers[8] first demonstrated three-dimensional manipulations of microparticles using only laser light. An optical tweezer is formed by tightly focusing a laser beam through an objective lens of high numerical aperture onto a particle. The movement and trapping of the particles along the beam axis are explained by considering two forces generated from the reflection and refraction of rays.[9] The two forces, the gradient force and the scattering force, are used to explain the dynamics of an optical trap. The scattering force is governed by the reflection of light incident on a particle and is also referred to as radiation pressure. The incident light reflects off the particle and exerts a force per unit area on the particle. Thus the scattering force pushes particles along the direction of light propagation. The gradient force, however, acts in the direction of the spatial intensity gradient, both laterally and axially. In order to obtain a stable three-dimensional trap, the gradient force in the axial direction must be greater than the scattering force, so as to overcome the radiation pressure. This requires a very steep intensity gradient, which is achieved by sharply focusing the laser beam on to a diffraction-limited spot by using an objective of high numerical aperture.

This article outlines the experimental set-up of an optical tweezer and how it can be utilised in measuring microscopic forces. By trapping particles using laser beams that carry angular momentum, optical tweezers may be used to not only demonstrate the rotation of particles, but also to measure the torque applied to the particles.

Linear and angular momentum

To visualise the forces involved in tweezing, consider the case where the particle size (a) is much larger than the wavelength (λ), $a >> \lambda$; the conditions for Mie scattering are satisfied and simple ray optics are used to calculate the forces involved in trapping. The gradient force can be explained in terms of conservation of momentum. As light is refracted through a transparent particle, there is a change in its direction and therefore a change in its momentum. According to Newton's third law of motion, the particle must undergo an equal and opposite change in momentum. The force that is experienced by the particle is simply the rate of change of the momentum, which is proportional to the intensity gradient of the beam. If the index of refraction of the particle is greater than that of the surrounding medium, the force as a result of refraction acts in the

direction of the intensity gradient (Figure 1). For a particle with a refractive index lower than that of the medium, the force acts in the opposite direction of the intensity gradient and tweezing is not achieved. An equivalent argument can be made for the case where $a << \lambda$, and one finds similar conclusions.[10,11]

Once a particle is trapped in three dimensions by the tweezer, it can be manipulated either by moving the laser beam with a steering mirror, thereby moving the particle, or by moving the surrounding untrapped particles by moving the sample stage. Repositioning the surrounding untrapped particles is a useful technique to determine the strength of the optical trap.

There are several different methods available to determine the strength of the trap. The choice of method depends on the availability of equipment and the degree of accuracy required. The following two methods were chosen based on availability of equipment, and both can be repeated easily without specialised equipment.

The first method makes use of the equipartition theorem to infer the strength of the trap. The energy equipartition theorem states that energy supplied by our thermal bath (the trapping environment) will be distributed equally across all degrees of freedom, each assigned a portion equal to $1/2\ k_B T$, where k_B is Boltzmann's constant and T is the equilibrium temperature of the bath. A particle held at some distance away from the focus of a trapping laser experiences an attractive force towards the focus. This restoring force is proportional to the displacement from equilibrium of the bead, that is, the trapping force of an optical tweezer can be thought of as an harmonic oscillator. According to Hooke's law:

$$F = -\alpha x, \qquad \text{[Eqn 1]}$$

F is the applied force, α is a constant referred to as the trap stiffness and x is the displacement. For an undamped system (i.e. a vacuum), an oscillator would have a resonant frequency of:

$$f_{res} = \frac{1}{2\pi}\left[\frac{\alpha}{m}\right]^{1/2}. \qquad \text{[Eqn 2]}$$

For a typical single cell, the frequency is thus f_{res} = 50 kHz. However, most optical trapping and tweezing of biological samples is not performed in a vacuum, but within an aqueous solution in order to keep the cell alive, resulting in a drag constant given by: $\beta = 6\pi R\eta$, where R is the radius of the particle and η is the viscosity of the solution. This damping, together with the stiffness of the trap, results in what is termed an 'over-damped system'. The bombardment of molecules of the surrounding medium results in a variance in displacement, $\langle x^2 \rangle$, of the trapped bead, which can be calculated from the equipartition of energy,

$$\frac{1}{2}\ \alpha\ \langle x^2 \rangle = \frac{1}{2}\ k_B T. \qquad \text{[Eqn 3]}$$

Experimentally, the only measurement needed is the centroid position of the trapped particle over some period of time in order to calculate the variance in the ensemble. By varying the power of the beam, we are changing the strength of the trap and therefore expect to see a change in the variance. From Hooke's law, the proportionality of the trap stiffness, α, and the force of the trap are clear. Therefore, from [Eqn 3], the variance of the particle's position must be inversely proportional to the force of the trap.

From the equipartition of energy theorem, we may infer the probability distribution of finding the trapped particle at a particular displacement, and this is given by the Boltzmann's distribution:

$$P(x) \propto \exp\left[\frac{-U(x)}{k_B T}\right] = \exp\left[\frac{-\alpha x 2}{2k_B T}\right] \qquad \text{[Eqn 4]}$$

where $U(x)$ is the potential energy and $k_B T$ is the thermal energy. As the gradient force is assumed to be a conservative force[12] (e.g. [Eqn 1]), the potential energy is the energy resulting from an object's position when it is acted on by a conservative force, and hence a potential energy distribution is expected, as given by [Eqn 4].

The second method takes into account that samples are predominantly viewed within a solution, and therefore

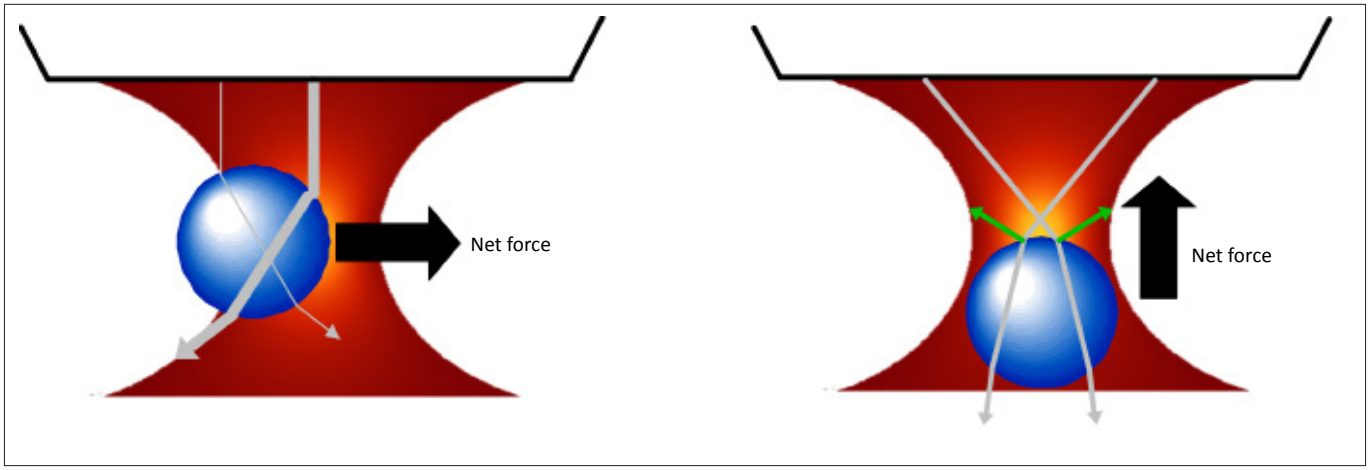

FIGURE 1: The refracted rays (grey) produce corresponding forces on the bead, resulting in a net force toward the most intense region of the beam. In the axial direction, the gradient force must be greater than the scattering force to obtain three-dimensional trapping.

any movement of a particle within the solution (fluid) will experience a drag force in the opposite direction of motion. The drag force, a force equivalent to friction, experienced by a particle in a fluid is given by:

$$F_{\text{Drag}} = 6\pi\eta R v, \qquad \text{[Eqn 5]}$$

where η is the viscosity of the fluid, R is the radius of the particle and v is the velocity of the fluid. This equation can be used to determine the trapping force by calculating the drag force that causes the particle to be released from the trap. That is, the velocity at which the particle escapes the 'hold' of the trap determines the drag force, which in turn determines the trapping force:

$$F_{\text{Trap}} = 6\pi\eta R v_{\text{c}}, \qquad \text{[Eqn 6]}$$

where v_{c} is the velocity of the fluid at which the particle escapes the trapping force.

Thus far, the forces discussed arise as a result of the transfer of linear momentum from the laser beam to the particle to be trapped. However, light may also transfer angular momentum to the particle. Additional trapping aspects can be attained by considering both the spin and orbital components of angular momentum. Spin angular momentum is associated with the polarisation state of light, whereas orbital angular momentum is related to the azimuthal phase of the light.

When polarised light passes through a birefringent material its polarisation changes. If the incoming light is left or right circularly polarised, and thereby carries spin angular momentum, then there will also be a change in its spin angular momentum, resulting in a torque on the material, causing it to rotate.[13,14] Light carries a spin angular momentum of $\sigma\hbar$ per photon, where $\sigma = 0$ for linearly polarised light and $\sigma = \pm 1$ for circularly polarised light, with the sign determined by the handedness of the polarisation (left or right). As light passes through a birefringent half-wave plate, the handedness of polarisation, and as a result angular momentum, is reversed. Each photon then transfers $2\hbar$ (because the momentum of the photons changes from $+\hbar$ to $-\hbar$, or $2\hbar$) of angular momentum to the plate, thereby exerting a torque on the plate. Friese et al.[15] demonstrated the transfer of spin angular momentum from a circularly polarised light beam to birefringent particles. As light passes through the particles, the ordinary and extraordinary components of the incoming light experience different phase shifts, resulting in a change in the angular momentum of the light. By comparing the angular momentum of the beam before entering and after exiting the trapped particle, the amount of spin angular momentum transferred to the particle can be calculated. The change in angular momentum generates a torque exerted on the particle, which has been previously measured by others.[15,16]

The other component of angular momentum of light, orbital angular momentum, is carried by beams with 'twisted' or helical wavefronts, unlike plane waves. Laguerre–Gauss beams fall into the category of beams known as vortex beams. In 1992, Allen et al.[17] showed that a Laguerre–Gaussian (LG) laser mode has a well-defined orbital angular momentum. The modes are commonly denoted by two indices: l is the number of 2π cycles in phase around the circumference, known as the azimuthal mode index, and $(p + 1)$ is the number of radial nodes. The amplitude of the LG mode has an azimuthal angular dependence of $\exp(-il\varphi)$. The LG modes are thought of as the eigenmodes of the angular momentum operator L_z[17], and so, carry an orbital angular momentum of $l\hbar$ per photon, where l is any integer. Allen et al.[17] presented a method to measure the angular momentum of a beam by measuring the torque acting on suspended cylindrical lenses as a result of the reversal of helicity of a LG beam, a similar experiment to that performed by Beth[13]. However, the first demonstration of the transfer of orbital angular momentum from a linearly polarised LG beam to absorbing particles was shown by He et al.[18] by making use of an optical trapping set-up. As the beam was linearly polarised with $\sigma = 0$, the rotation of the trapped particles caused by the transfer of angular momentum demonstrated the transfer of orbital angular momentum.

When measuring the torques experienced by the particles as a result of the transfer of angular momentum, a similar drag force method is used, which can be applied to both components of angular momentum. As previously stated, birefringent materials in general cause the polarisation to change and correspondingly, the angular momentum of the beam changes. The torque is equal to the change in angular momentum flux, given by

$$\tau = \frac{(\sigma_{\text{in}} - \sigma_{\text{out}})P}{v}, \qquad \text{[Eqn 7]}$$

where σ_{in} and σ_{out} denote the incident and outgoing polarisation coefficients, respectively, P is the total power carried by the laser to the particle and v is the frequency of the light. In a viscous medium, a drag torque, $\tau_{\text{D}} = D\Omega$, is present, which at equilibrium will balance the exerted torque, where D is the drag coefficient and Ω is the angular frequency of rotation. For a sphere rotating in a medium of low Reynolds number, the drag torque is given by

$$\tau_{\text{D}} = 8\pi\mu a^3\Omega, \qquad \text{[Eqn 8]}$$

where μ is the viscosity of the medium and a is the radius of the sphere. As the exerted and drag torques are balanced, they can be equated to solve for any of the parameters which are unknown. For example, the viscosity of the medium is not always known or the medium itself is unknown, and so equating [Eqn 7] and [Eqn 8] gives

$$\mu = \Delta\sigma P/(8\pi a^3\Omega v). \qquad \text{[Eqn 9]}$$

Using the aforementioned optical tweezing methods, we are able to demonstrate the transfer of both linear and angular momentum of light to microscopic particles and, in turn, to quantify the forces and torques experienced on the microscopic level.

Measuring microscopic forces and torques

The experimental design and set-up of the optical tweezer (Figure 2) was based on set-ups presented in previous reviews.[19,20,21] The beam was expanded through a 3x telescope, f_1 = 30 mm and f_2 = 100 mm, before it was reflected off the dichroic mirror onto the back aperture of the 100x objective lens. The dichroic mirror transmits light between 455 nm and 650 nm, allowing the laser light (λ = 660 nm) to be reflected, whilst transmitting light from the white light LED illumination source. A 100x objective (model LA-MA-OB-EAB100, LOMO Inc., USA) with a numerical aperture of 1.25, working distance of 0.17 mm, tube length of 160 mm and oil immersion was used. A field lens of focal length f = 150 mm was placed 160 mm above the objective lens, directing the image onto the camera. A Scorpion IEEE-1394 camera (model SCOR-20SO, Spiricon Inc., USA) was used with a resolution of 1600 x 1200 pixels with a pixel size of 4.4 µm x 4.4 µm.

Silica beads with a mean diameter given as 4.32 µm and a refractive index of n = 1.44 (Bangs Laboratory Inc., USA) were placed in distilled water (refractive index of 1.33), at a concentration of 0.5 mg/mL. The silica beads have a low absorption at the laser wavelength, and hence are ideal for studying the transfer of linear momentum, that is, refraction-only regimes.

In the first experiment to measure the forces as a result of the transfer of linear momentum, the centroid position of a trapped bead was recorded (over 100 frames of the camera) and the variance calculated. The power of the laser was varied using neutral density filters and the variance of the bead was calculated at each power. We expected an inversely proportional relationship between the beam power and the variance of the particle's position, because strongly trapped particles (high power) have less freedom to move than weakly trapped particles (low power), whereas we expected a linear relationship between the trap strength and the trap stiffness. Figures 3 and 4 illustrate these expected relationships between the trap strength (power of beam) and the variance of the particle position and trap stiffness, respectively.

For the lowest power, a value of $9.9 \times 10^{-5} \pm 5 \times 10^{-6}$ N/m for the trap stiffness was obtained. The trends obtained are in agreement with theory, whilst the values are in the same range as that found previously.[22]

Using the same variance data as above, the distribution of bead positions can be plotted with a fitted curve using [Eqn 4], and is shown in Figure 5. The fitted curve allows the trap stiffness to be determined, where $k_B = 1.38 \times 10^{-23}$ m^2kg/s^2K^1 and T = 300 K. The trap stiffness at the lowest measured power was determined to be $\alpha = 8.7 \times 10^{-5}$ N/m, which corresponded quite well with the value calculated at the same power using the variance method of $\alpha = 9.9 \times 10^{-5}$ N/m. The potential energy curve was obtained from the position distribution and clearly shows a parabolic shape

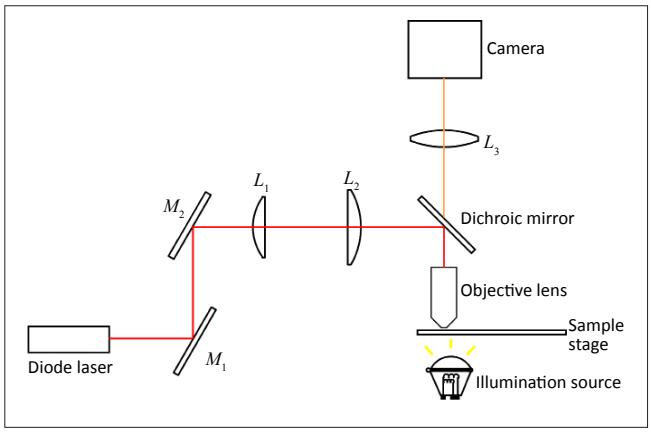

FIGURE 2: Diagram of the experimental set-up used to produce an optical trap. The beam is emitted from the Diode laser, reflected off mirror M_1 to mirror M_2 and expanded through lenses L_1 and L_2 before it is reflected off a dichroic mirror onto the back aperture of an objective lens. The sample is illuminated from below by a white light LED source and imaged to a charge-coupled device (CCD) camera placed above the system by a field lens L_3.

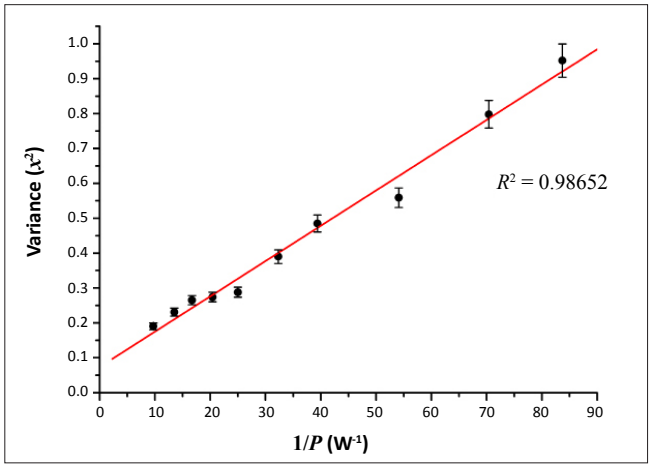

FIGURE 3: Graph illustrating the inverse relationship between the variance of the position of a trapped bead and the power of the applied laser beam.

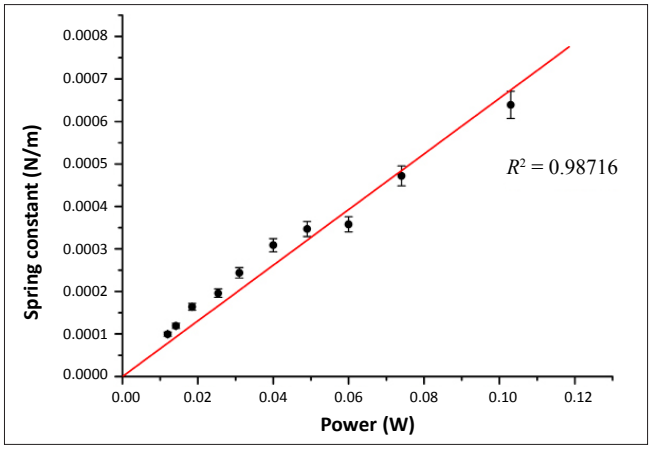

FIGURE 4: Graph illustrating the linear relationship between the spring constant of the trap and the power of the applied laser beam.

(Figure 6). A trapped particle will therefore remain trapped at its equilibrium position unless it gains enough energy to escape the potential well.

The second method, using the drag force acting on the bead, produced similar results. Once a bead was trapped, the stage

was moved with increasing speed and the displacement of a reference bead, one that was stuck to the glass slide, was monitored. The displacement of the reference bead just as the trapped bead had escaped was then determined and, by using the time between each frame, the velocity was calculated. The frame rate of the camera was set at 15 frames/s, therefore the time difference (Δt) between consecutive frames was approximately 67 ms. The velocity of the fluid as the bead escaped was calculated using

$$v_c = \frac{\Delta x}{\Delta t}. \qquad \text{[Eqn 10]}$$

From [Eqn 10], the escape velocity was calculated to be $v_c \approx 36$ µm/s, resulting in an escape force of $F_{Trap} \approx 1.5$ pN. This calculation was performed at a number of different incident powers, where neutral density filters were used to reduce the power of the beam. The actual power delivered to the trap was difficult to measure because of the fast divergence of the beam. Therefore relative power measurements were made by measuring the power before it entered the objective.

The maximum force acting on the bead for this particular method was calculated to be 5.2 ± 0.3 pN at a power of P = 100 mW, as shown in Figure 7. Improving the accuracy of this measurement is the subject of ongoing research in this field; for review see Neuman and Block[20].

Measurement of the microscopic torques experienced by the particles required a few alterations to the original optical tweezer set-up. Linearly polarised lasers require a quarter-wave plate to be inserted into the set-up to change to circularly polarised light, and the silica beads in distilled water were replaced with calcite particles in ethanol. Calcite particles were chosen for their well-known birefringence. The frame rate of the camera was set to 15 frames/s, which allowed the time between the number of frames to be calculated. The angular speed at which the trapped particle rotated was calculated using

$$\omega \approx \frac{\Delta\theta}{\Delta t}, \qquad \text{[Eqn 11]}$$

where $\Delta\theta$ is the change in angular position of the particle within time Δt. Figure 8 shows the particle rotating in an anticlockwise direction, with the time between each of the frames being ~1 s. It is clear that the particle rotated by an angle of 1.6 rad between each of the frames, therefore, according to [Eqn 11], $\omega = 1.6 \pm 0.1$ rad/s. The wave plate was then rotated by 90°, causing the polarisation to change handedness; the particle was seen to rotate but in a clockwise direction, as shown in Figure 9. The results in Figures 8 and 9 clearly illustrate the left-handedness and right-handedness of spin angular momentum. Again, the angular speed of rotation was calculated to be $\omega = 1.6 \pm 0.1$ rad/s, which is expected, as the direction of polarisation was the only variable to change. Using [Eqn 8], it is possible to calculate the torque exerted on the calcite particle. The viscosity of ethanol is $\mu = 1.1 \times 10^{-3}$ Ns/m^2, the radius of the particle is approximately $a \sim 1$ µm and the angular frequency of rotation is calculated as $\Omega = \omega / 2\pi = 0.25$ Hz. Using these values, a torque of $\tau = 8 \times 10^{-21} \pm 0.4 \times 10^{-21}$ Nm was obtained.

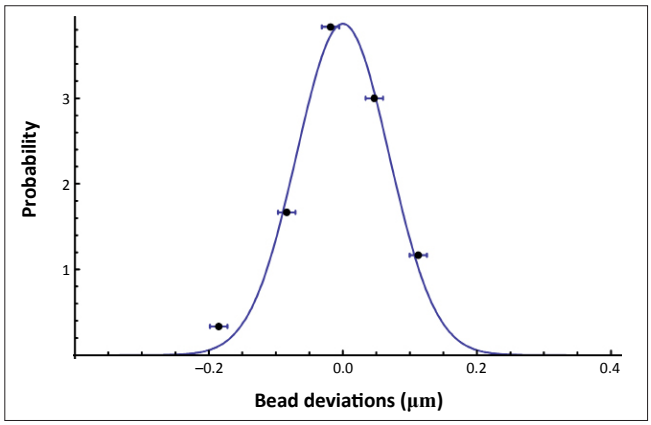

FIGURE 5: Graph representing the distribution of bead positions. A Gaussian function is fitted to the measured data points using [Eqn 4].

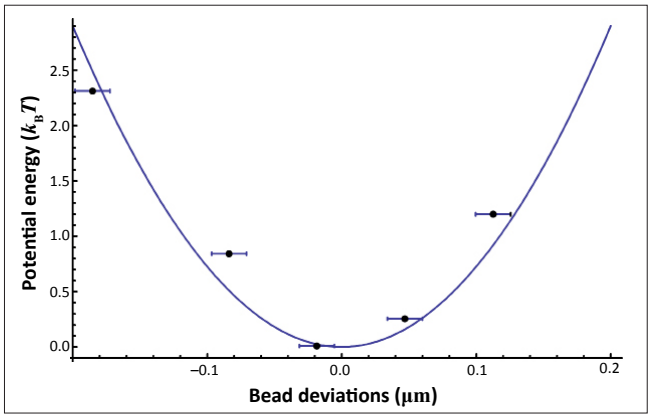

FIGURE 6: Graph representing the potential energy calculated from the distribution of bead positions. A quadratic function is fitted to the measured data points using [Eqn 4].

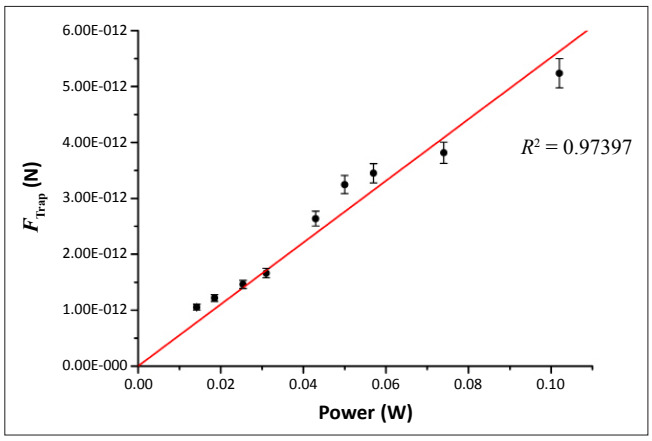

FIGURE 7: Graph illustrating the linear relationship between the trapping force on the bead and the power of the applied laser beam.

The same calculations can be applied to particles rotating as a result of a transfer of orbital angular momentum. The experimental set-up, however, requires additional elements in order to produce LG beams. The most commonly used method involves a spatial light modulator, which allows beam shaping to be performed quickly and efficiently. Figure 10 shows the changes made to the experimental set-up, where a spatial light modulator has been introduced for the creation of the vortex beam. The vortex beam (a ring of light with a dark centre) was created by programming an

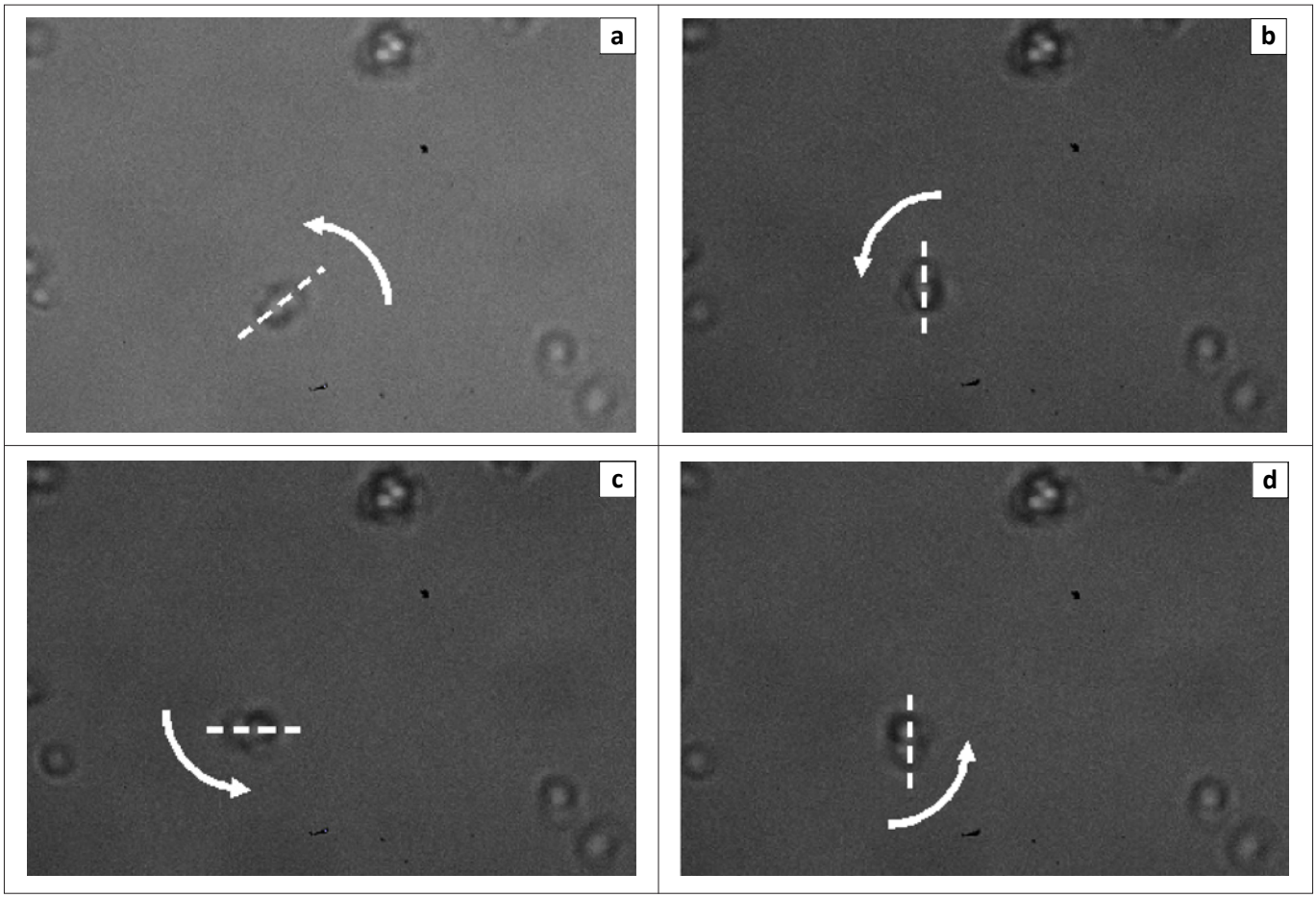

FIGURE 8: Images of birefringent calcite particles in ethanol showing a particle rotating in an anticlockwise direction (a–d) at a rate of $\omega = \pi/2$ rad/s.

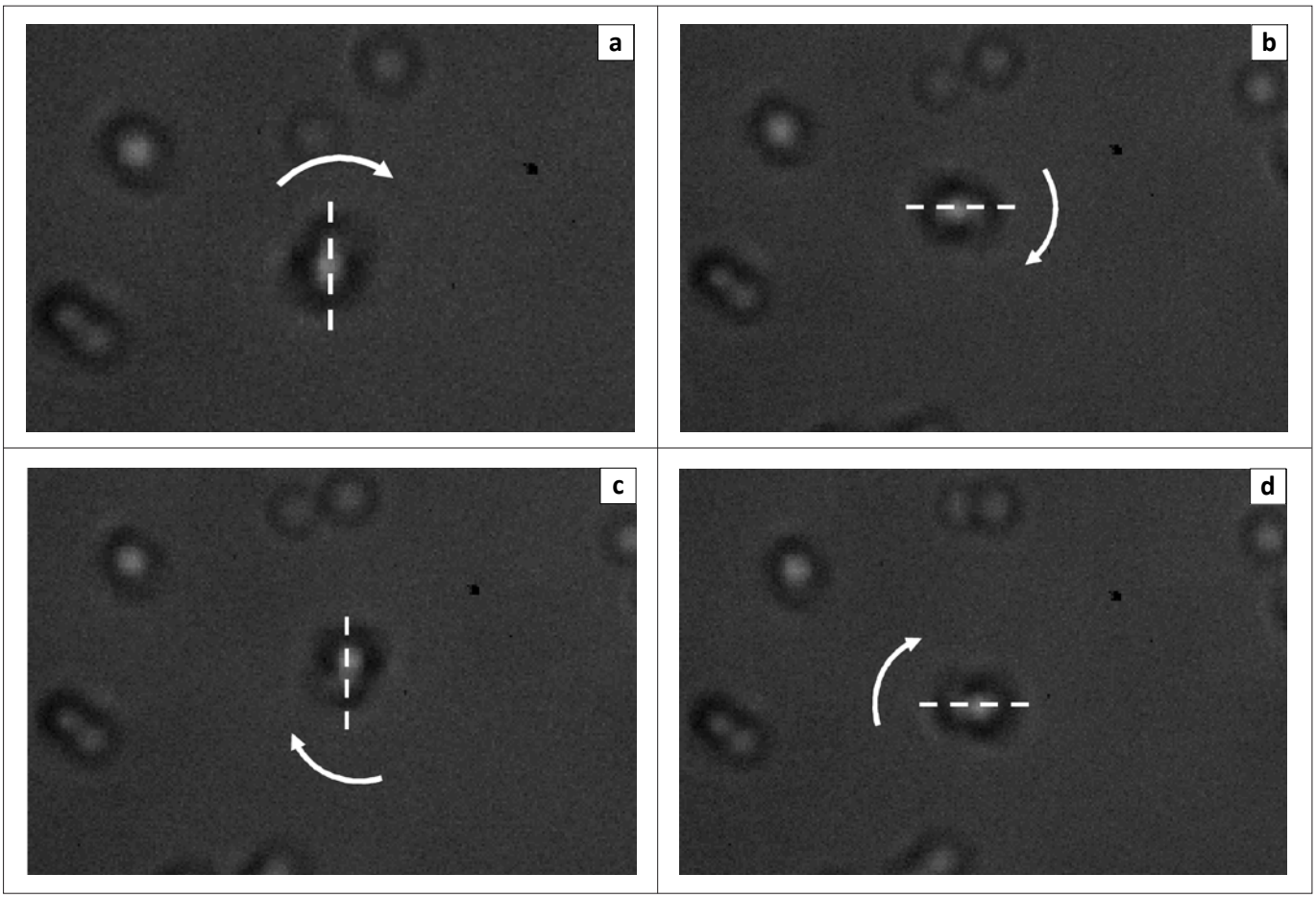

FIGURE 9: Images of birefringent calcite particles in ethanol showing a particle rotating in a clockwise direction (a–d) at a rate of $\omega = \pi/2$ rad/s.

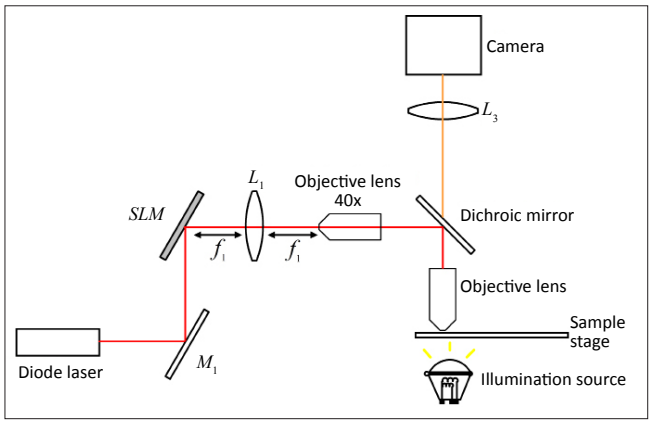

M_1, mirror; f_1, focal length; L_1, telescope lens; L_3, field lens.

FIGURE 10: Experimental set-up used for rotating particles about a point. A spatial light modulator (SLM) is used to generate a vortex beam, which carries orbital angular momentum.

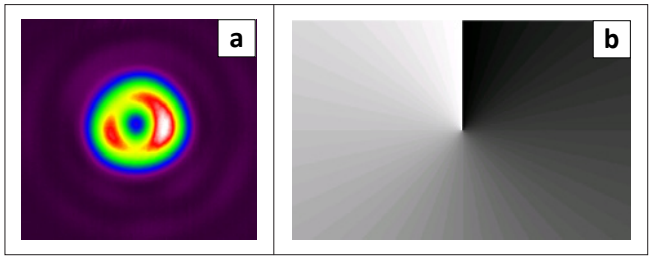

FIGURE 11: (a) Image of a vortex beam with l = 1, showing the intensity distribution. (b) A greyscale phase pattern encoded with an azimuthal phase was used to convert the incoming Gaussian laser beam to the vortex beam.

azimuthal phase pattern onto the spatial light modulator in the form of a greyscale image, representing a phase change to the incoming beam from 0 (white) to 2π (black) in steps of 2π/255 (greyscale). An experimental image of the vortex beam is shown in Figure 11, together with the greyscale image that created it. In this particular experiment, graphite particles of non-uniform size were suspended in distilled water and exposed to a vortex beam of order l = 1. The particles were trapped in the dark centre of the beam and subsequently began to rotate in an anticlockwise direction (Figure 12). Using the same method as previously described, the angular speed was calculated to be approximately $\omega \approx 3$ rad/s, giving a rotational frequency of $\Omega = 0.5$ Hz. A torque of $\tau = 1.2 \times 10^{-20} \pm 0.2 \times 10^{-20}$ Nm was calculated.

Discussion and conclusion

We have outlined the basic principles of an optical trapping and tweezing system, and shown how the system may be characterised through the measurement of microscopic forces and torques. These results are a prerequisite for a number of applications, particularly in biology and chemistry, which require precise and accurate control (movement, placement, etc.) at the microscopic scale. Thus, whilst this article has concentrated on the method of optical trapping and tweezing, and the careful characterisation of the forces and torques involved at the microscopic level, it would be remiss of us not to comment on the vast applications of such a technique.

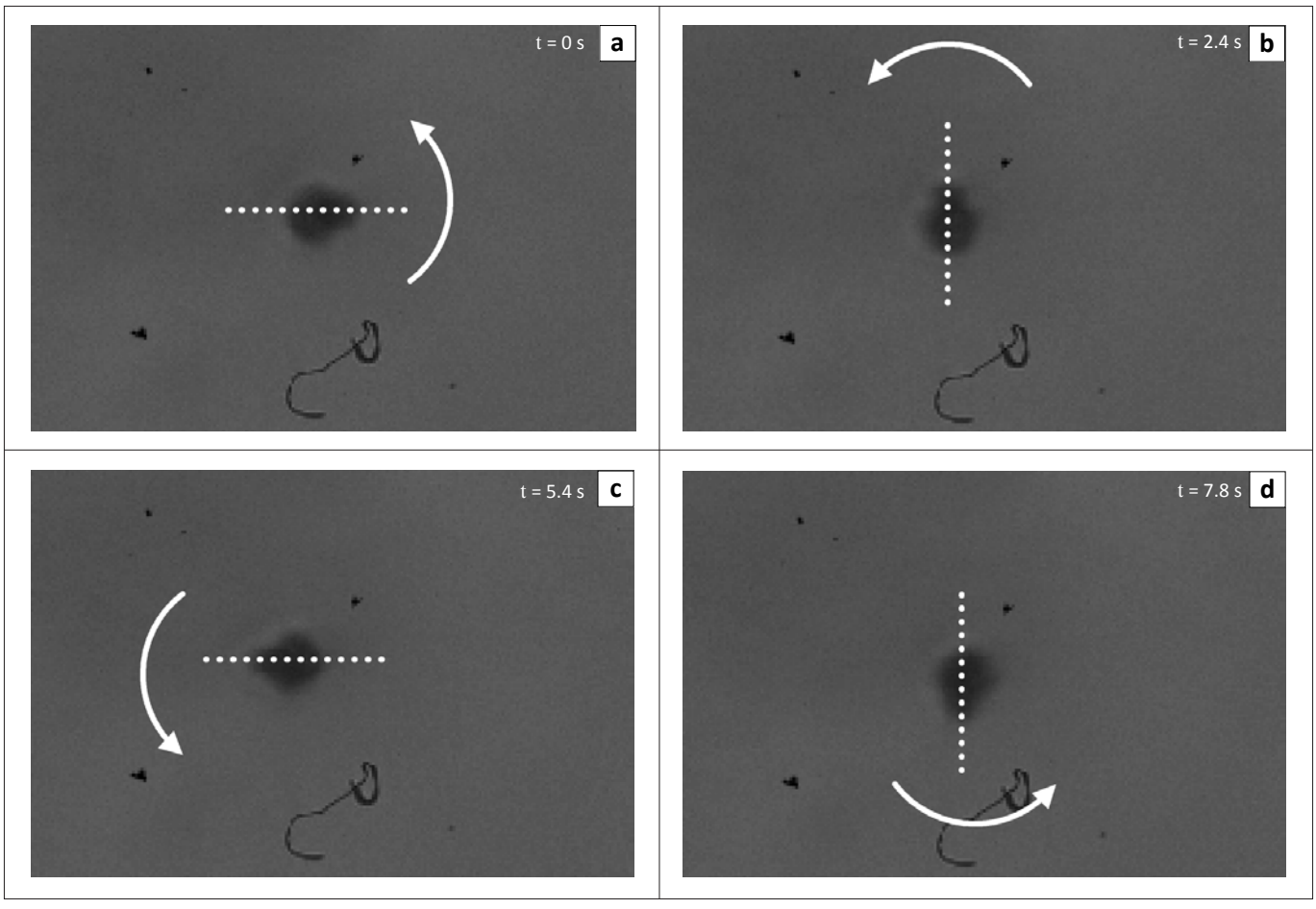

FIGURE 12: A graphite particle of 1-μm diameter was exposed to the vortex of order l = 1. The particle rotated in a clockwise direction (a–d) at a frequency of approximately 0.5 Hz.

The continuous development of optical tweezers over the past 30 years has resulted in immense interest within a number of different research fields. In particular, the non-invasive quality of optical tweezers (with the ability to manipulate biological cells in a controlled manner without harming the cell) has attracted attention from those dealing with biological materials. In particular, the pico-Newton forces of optical tweezers allows the mechanical properties of molecular motors and biopolymers to be measured.[1] Biological research also makes use of trapped beads (as we have done in this study) by attaching a biological structure to the trapped bead, thereby using the bead as a 'handle' of sorts for control by the laser beam, for example, in studying curvature-dependent interactions with associated proteins in long DNA strands.[2] Optical tweezers have also been useful in stimulating neuronal growth[3,4] and in sorting blood cells (red and white) based on their size difference.[21]

Another field of research that is gaining a great deal of attention is microfluidics.[5] A microfluidic system often refers to a channel system where at least one dimension is on the order of micrometers. These systems are sometimes replicas of macroscale devices and therefore microfluidics is regularly termed 'lab-on-a-chip'. When working on such a small scale, certain properties alter, making some experiments easier to perform than at macroscopic scales. That is, at the microscopic scale, the surface-to-volume ratio increases considerably, causing the flows within the system to be almost laminar.[5] Therefore two different solutions can flow next to one another without mixing for as long as a few minutes. Optical tweezing has been used to trap a particle in one flowing solution and move it across to the neighbouring solution for the purpose of examining the effects of various solutions on a particle.[6] The technique is efficient and reversible, allowing particles to be moved from one solution to another and finally returning them to the original solution with ease.

The implementation of transferring angular momentum to particles within an optical trap has opened up a diverse range of applications within microfluidics: trapped spherical particles offer an effective method of determining unknown parameters of the fluid. As previously mentioned, by measuring the rotation frequency of a particle of known size and the change in polarisation, the viscosity of the fluid can be calculated. Similarly, the radius of the particle can be determined if the other parameters are known. The transfer of angular momentum within microfluidic channels has also been used to convert laminar flow to turbulent flow, for mixing, as well as to drive the flow in the channels. In one example, two spherical vaterite (CaCO3) particles, trapped next to each other, were rotated in opposite directions, thereby forming an optical micropump: a constant flow between the particles formed, forcing untrapped particles to follow the resulting flow.[23] The transfer of angular momentum within an optical trap has also been used to drive microgears, where the light is a form of optical spanner.[16,24]

Optical trapping and tweezing has opened the way for all-optical control within microfluidic devices: from driving the flow and measuring the flow to manipulating trapped species within the devices. As such, optical trapping and tweezing is proving a versatile tool across many disciplines. We have thus outlined the basic steps needed to build and characterise such a device for the control of microscopic objects using the transfer of momentum of light.

References

1. Kuyper CL, Chui DT. Optical trapping: A versatile technique for biomanipulation. Appl Spectrosc. 2002;56:300A–312A. doi:10.1366/00037020260377652
2. Arai Y, Yasuda R, Akashi K, et al. Tying a molecular knot with optical tweezers. Nature. 1999;399:446–448. doi:10.1038/20894, PMid:10365955
3. Ehrlicher A, Betz T, Stuhrmann B, et al. Guiding neuronal growth with light. Proc Natl Acad Sci USA. 2002;99:16024–16028. doi:10.1073/pnas.252631899, PMid:12456879, PMCid:138558
4. Carnegie DJ, Stevenson DJ, Mazilu M, et al. Guided neuronal growth using optical line traps. Opt Express. 2008;16:10507–10517. doi:10.1364/OE.16.010507, PMid:18607464
5. Squires TM, Quake SR. Microfluidics: Fluid physics at the nanoliter scale. Rev Mod Phys. 2005;77:977–1026. doi:10.1103/RevModPhys.77.977
6. Eriksson E, Enger J, Nordlander B, et al. A microfluidic system in combination with optical tweezers for analyzing rapid and reversible cytological alterations in single cells upon environmental changes. Lab Chip. 2007;7:71–76. doi: 10.1039/B613650H
7. Hopkins RJ, Mitchem L, Ward AD, Reid JP. Control and characterisation of a single aerosol droplet in a single-beam gradient force optical trap. Phys Chem Chem Phys. 2004;6:4924–4927. doi:10.1039/b414459g
8. Ashkin A, Dziedzic JM, Bjorkholm JE, Chu S. Observation of a single-beam gradient force optical trap for dielectric particles. Opt Lett. 1986;11:288–290. doi:10.1364/OL.11.000288, PMid:19730608
9. Ashkin A. Acceleration and trapping of particles by radiation pressure. Phys Rev Lett. 1970;24:156–159. doi:10.1103/PhysRevLett.24.156
10. Rohrbach A, Stelzer EHK. Trapping forces, force constants, and potential depths for dielectric spheres in the presence of spherical aberrations. Appl Opt. 2002;41:2494–2507. doi:10.1364/AO.41.002494, PMid:12009161
11. Smith S, Bhalotra S, Brody A, Brown B, Boyda E, Prentiss M. Inexpensive optical tweezers for undergraduate laboratories. Am J Phys. 1998;67:26–35. doi:10.1119/1.19187
12. Ashkin A. Forces of a single-beam gradient laser trap on a dielectric sphere in the ray optics regime. Biophys J. 1992;61(2):569–582.
13. Beth RA. Mechanical detection and measurement of the angular momentum of light. Phys Rev. 1936;50:115–125. doi:10.1103/PhysRev.50.115
14. Poynting JH. The wave motion of a revolving shaft, and a suggestion as to the angular momentum in a beam of circularly polarised light. Proc R Soc Lond A. 1909;82:560–567. doi:10.1098/rspa.1909.0060
15. Friese MEJ, Nieminen TA, Heckenberg NR, Rubinsztein-Dunlop H. Optical alignment and spinning of laser-trapped microscopic particles. Nature. 1998;394:348–351. doi:10.1038/28566
16. Simpson NB, Dholakia K, Allen L, Padgett MJ. Mechanical equivalence of spin and orbital angular momentum of light: An optical spanner. Opt Lett. 1997;22:52–54. doi:10.1364/OL.22.000052, PMid:18183100
17. Allen L, Beijersbergen MW, Spreeuw RJC, Woerdman JP. Orbital angular momentum of light and the transformation of Laguerre–Gaussian laser modes. Phys Rev A. 1992;45:8185–8189. doi:10.1103/PhysRevA.45.8185, PMid:9906912
18. He H, Friese MEJ, Heckenberg NR, Rubinsztein-Dunlop H. Direct observation of transfer of angular momentum to absorptive particles from a laser beam with a phase singularity. Phys Rev Lett. 1995;75:826–829. doi:10.1103/PhysRevLett.75.826, PMid:10060128
19. Fischer P, Little H, Smith RL, et al. Wavelength dependent propagation and reconstruction of white light bessel beams. J Opt A: Pure Appl Opt. 2006;8:477–482. doi:10.1088/1464-4258/8/5/018
20. Neuman K, Block S. Optical trapping. Rev Sci Instrum. 2004;75:2787–2809. doi:10.1063/1.1785844, PMid:16878180, PMCid:1523313
21. Dholakia K, Reece P, Gu M. Optical micromanipulation. Chem Soc Rev. 2007;37:42–55. doi:10.1039/b512471a, PMid:18197332
22. Bechhoefer J, Wilson S. Faster, cheaper, safer optical tweezers for the undergraduate laboratory. Am J Phys. 2001;70:393–400. doi:10.1119/1.1445403
23. Leach J, Mushfique H, Di Leonardo R, Padgett M, Cooper J. An optically driven pump for microfluidics. Lab Chip. 2006;6:735–739.
24. Neale SL, MacDonald MP, Dholakia K, Krauss TF. All-optical control of microfluidic components using form birefringence. Nat Mater. 2005;4:530–533. doi:10.1038/nmat1411, PMid:15965480